JOINT EUROPEAN TORUS

JET–P(95)68

Many Authors

JET Papers presented to the 2nd Workshop on Electrical Probes in Magnetised Plasmas (Berlin, Germany, 4-6 October 1995)

JET Papers presented to the 2nd Workshop on Electrical Probes in Magnetised Plasmas (Berlin, Germany, 4-6 October 1995)

Many Authors

JET-Joint Undertaking, Culham Science Centre, OX14 3EA, Abingdon, UK

Preprint of Papers to be submitted for publication in
Contributions to Plasma Physics (Probe Workshop, Berlin).

November 1995

JET Papers presented to 2nd Workshop on Electrical Probes in Magnetised Plasmas (Berlin, Germany, 4–6 October 1995)

Contents

Technical Performance of Fixed Langmuir Probe Systems in the JET Pumped Divertor

G.F.Matthews, S.J.Davies and R.D.Monk[1]

JET Joint Undertaking,Abingdon,Oxforshire,OX14 3EA
[1]Dept. of Physics, Royal Holloway College,University of London, Surrey,TW20 OEX,UK

Abstract. In this paper, the new fixed Langmuir probe systems developed for the Mark I pumped divertor phase of JET are described along with the plans for the new Mark II divertor probe systems. The system installed in Mark I consisted of 22 limiter probes plus 149 divertor probe tips configurable as 149 single Langmuir probes or as 39 triple probes plus 32 single probes. A VME based data acquisition system was developed which acquired data from all probes simultaneously at a rate of 5KHz (342 channels). The concept of the "hands-off" intelligent probe system and its realisation are described. In contrast to previous probe designs, after one year of operation, the pyrolitic graphite probe tips showed very little sign of erosion. Possible reasons for this important advance are presented. Plans for a "pop-up" probe system in the new Mark II divertor are outlined which will be used to expose less robust pin-plate probes to the plasma which would not survive permanent exposure. It is hoped that pin-plate probes will allow the elimination of the effects of plasma resistivity from the interpretation of single probe characteristics.

1. Introduction

This paper aims to describe the technical design and performance of the fixed probe system which was implemented in JET Mark I pumped divertor. Details of the data produced by this system and the analysis procedures applied can be found in the companion paper by Monk et al. [1].

The probe design used in JET up until the installation of the pumped divertor proved very valuable for divertor physics and was essentially duplicated on JT60 and DIII-D. These probe tips were domed and protruded through holes in the target tiles as shown in figure 1. Fine grained graphite was used along with alumina insulators. The final installation consisted of 16 single Langmuir probes in the upper and lower X-point tiles. Data acquisition was via standard CAMAC modules to which selected probes were connected via a manual patch panel. Unfortunately, most of the probes ceased to function after the first few weeks of high power operations. Replacement was not easy since the beryllium hazard means that all in-vessel work required the use of pressurised suits and whole tiles had to be removed to get at the probes. The data acquisition was also not ideal requiring constant supervision of time windows and the patch panel was prone to human error.

Figure 1. Original JET probe design used until 1992.

Failures of the original probes were due to two separate causes. Firstly, the thermal characteristics of the probes were worse than those of the tiles in which they were mounted because of the inferior thermal properties of the probe material and a less favourable geometry. Since carbon blooms were a common feature of JET operation at this time it is not perhaps suprising that many probe tips were completely vaporised. There is also evidence that high tile temperatures, coupled with large fluxes of atomic hydrogen, caused the alumina (Al_2O_3) insulators to be reduced to aluminium so that conducting films developed. The leakage resistance of many probes decreased with time sometimes reaching an unacceptably low level. After a vent however the resistance jumped back to a very high level consistent with oxidation of an aluminium film.

Even when the probes were functioning, there were analysis problems associated with non-saturation of the ion current [2]. This problem was first identified on DITE where it was shown that non-saturation can occur when the angle of incidence of the magnetic field to the probe surface is less than 10° [2].

Given this previous experience the design goals for the new probe system for the pumped divertor were: A probe tip which was thermally superior to the target. Probe projected dimensions large compared the ion gyro-radius and an angle of incidence in excess of 10° to avoid the problems of flush mounted probes. No alumina insulators. Intelligent control and data acquisition requiring minimal human intervention.

2. Mark I Probe Design

The Mark I pumped divertor consisted of 48 modules. Each of the modules shown in figure 2 had four water cooled beams on which sprung loaded tile pairs were located. Between each successive row of tile pairs were toroidal gaps which tapered from 10.2 to 12.4mm as one moved from the inner to the outer corner of the divertor trough. The probes were located in these gaps as shown in figure 3. Only one helicity of the magnetic field was allowed for by the divertor tiles which were shingled to avoid any exposure of the edges.

Figure 2. Mark I pumped divertor structure with some tiles removed to show support beams.

The probe assemblies were mounted on cable conduits which were attached to the tile support beams. Details of the probe assembly are shown in figure 3. Allowance was made in the design for vertical and toroidal adjustment of the probe tips so that the height of the tip above the tiles and the separation from their rear faces could be accurately set. Pyrolitic boron nitride insulators were used and included multiple labyrinth features to resist accumulation of conducting deposits.

Fine grained graphite of the type used in the original JET probes has a room temperature thermal conductivity $k=100Wm^{-1}K^{-1}$. The materials selected to make the Mark I probes were 3D fine weave carbon fibre composite with $k=161Wm^{-1}K^{-1}$ in the best conductivity direction and pyrolitic graphite with $k=350Wm^{-1}K^{-1}$ parallel to the plane of good conductivity. The probe tip itself is a miniature shingle which is set so that its leading edge is never exposed and is slightly parallelogramed to minimise plasma interaction with the sides due to the radial component of the poloidal field, this arrangement is illustrated by figure 4.

Figure 3. Mark I divertor probe assembly.

Figure 4. The relationship between the probe tip and tile.

A sensitivity analysis of the range of anticipated magnetic equilibria linked with a consideration of installation tolerances led to a choice of 11°(with respect to the horizontal) for the probe surface angle which should be compared with the 4° angle of the target tile. This guarunteed a projected height of 1-2mm which combined with the 2.5mm width gave a typical area in the region of $4mm^2$.

Compounded with a typical magnetic field angle to the horizontal of 5°, the probe and surface angles implied a typical power density enhancement to the probe surface of 1.75. There was potential for this to be enhanced further due to the input from the probe power supplies which in principle could deliver up to $30MWm^{-2}$. These disadvantages were offset by expanding the root of the probe below the line of sight of the plasma thus providing the tip with a local heat sink. ABAQUS [3], a finite element code which is applicable to the transient thermal analysis, was used to demonstrate the benefits of this geometry and of the pyrolitic graphite. Time to reach sublimation temperature for various probe materials is plotted as a function of surface power density in figure 5. At low power densities, all probes perform better than the 1D tile model due to the heat sink effect of the probe root. At sufficiently high power however, the lines converge due to the fact that the heat pulse has insufficient time to penetrate to the probe root. In this limit of very high power densities only the pyrolitic graphite probes outperform the tiles due to the superior thermal properties. These calculations were verfied experimentally by exposing sample probe tips in the JET neutral beam test bed.

Figure 5. Finite element calculations for the time taken for the probe tip surface to reach sublimation temperature for a range of materials.

3. Configuration, Control and Data Acquisition

The probe configuration was limited by the available electrical feedthroughs to two sets of 16 single Langmuir probes in octants 2 and 6 plus an array of 39 triple probes in octant 5. In addition there were 22 single probes distributed over the inner and outer limiters. Triple probes have the advantage that the data are easy to analyse and can offer very high time resolution subject to the limitation that all three probe tips are exposed to the same plasma conditions [2]. The three probe tips comprising the JET triple probes were distributed toroidally at the same major radius in successive slots. Toroidal uniformity has not proven a problem in JET and the triple probe technique works well [1]. There is no evidence of cross-talk between adjoining probe tips except at very low field angles.

Power to the triple probes was provided by full wave rectified isolated transformers which were rated at 3A and output up to 160V. The thermal inertia of these transformers was sufficient to allow 10A to be driven for at least 30s, more than enough to melt the wiring in the vacuum feedthrough. The peak design current was 10A but supplies were fused to limit the duration sufficient to protect the feedthroughs. A system of relays was employed to allow the triple probes to be reconfigured as single probes or floating single probes under remote control. Swept voltage was provided to all single probes by two switched mode power supplies the larger of which had a 38A, ±200V capability.

To meet the design requirement that there be no patching 342 isolated 16 bit ADC channels were used to record the current and voltage data from the 171 probe tips at 5KHz which generated 3.4Mb s^{-1}. In order to avoid manual selection of time windows data had to be taken for at least 20s which required that 70Mb of data per pulse were dealt with. This is double the total amount of data stored per pulse by all JET systems in 1992. A solution based on standard CAMAC modules was thus not possible and so a VME based system was employed instead. This consisted of 6 Texas Instruments C40 digital signal processors, with 8Mb of memory, each of which controlled 16 8 channel 16 bit ADCs.

Fortunately, except during events such as ELMs or disruptions, probes located far from the strike points saw signal levels below the noise level. For this reason, a simple real-time data reduction algorithm based on setting a threshold below which data was not stored was implemented in the C40s and reduced the mean data volume by more than an order of magnitude. This has meant that all probes were permitted to take data at the maximum rate for the whole pulse and will allow the system to be upgraded for 10KHz sampling.

Control of the system was essentially fully automatic involving the following steps:

Pre-pulse checks - Calibrate current and voltage circuits. Look for blown fuses and test probes for short circuits.

If faults found - Display status on mimic (graphical representation of probe system). Re-configure faulty triple probes as single probes

During the pulse- Digitise data on all 342 channels at 5khz. Check for arcs and temporarily power down affected triple probes to extinguish the arc. Start data reduction removing redundant data and signals close to the noise level.

Post-pulse: Complete data reduction and ship data to Jet Pulse File (JPF). Repeat fuse checks and update mimic including any arcs which were detected.

Due to the constant bias on the triple probes, once struck, arcs were sometimes produced which would keep burning until the fuses blew. During disruptions, or large ELMs, tens of fuses would often blow, predominantly associated with the inner target triple probes. This problem was overcome by using the C40 processors to monitor the triple probes and temporarily power down any which show high currents.

4. Lifetime of the Mark I probe tips

After one year of operation around 70% of the probes were still operational with no obvious degradation of probe area. Most of the failures appear to have been caused by inadequate protection during in-vessel interventions. Those that survived the feet showed no sign of thermal sublimation. The only significant change in appearance was a slight rounding of the corners amounting to about 0.1mm. This change should be compared with an estimated deuteron fluence of $1\text{-}2\times10^{27}m^{-2}$. If redeposition is ignored, which seems reasonable for sharp edges, this implies a sputtering yield of 1-2% which is consistent with physical sputtering. The chemical sputtering yield would be expected to be around 10% and so if this played a role severe erosion should have been observed. However, this result merely confirms colorimetric measurements of target tile erosion [4] which showed that chemical sputtering was suppressed in high flux regions of the target.

5. Mark II Probe Systems

Although the Mark II divertor which is currently being installed in JET represents a major change in structure to a more closed geometry with large format tiles, the design of the fixed probe system remains very similar to that employed in Mark I. However, because there can be significant bowing of the tiles due to thermal expansion the probes are attached to the rear face of the tiles.

In addition to the fixed probes there will be two "pop-up" probe systems located in the inner and outer divertor regions, as shown in figure 6. These use a moving coil to raise a row of probes by 5mm in 10ms. This is sufficient to move the probe tips from the shadow of the tiles to an exposed position. This system was developed as insurance against the possibility that the fixed probe tips suffered significant erosion damage. Experience with the Mark I probes suggests that this is unlikely to happen and so a new role has been found in the insertion of relatively vulnerable pin-plate probes into the divertor plasma.

Figure 6. Mark II divertor structure and location of "pop-up" probe systems.

Pin-plate probes are a concept proposed by Stangeby [5] to provide a technical solution to the problem of plasma resistivity. The usual probe interpretation assumes that all the measured potential is dropped across the probe sheath but in reality this is not always the case [6]. High plasma resistivity leads to an overestimate of the potential at the probe sheath edge and so an overestimate of the electron temperature. Unfortunately, the problem of cross-field current flow appears so complex that it is any unlikely that it will ever be possible to use resistive plasma theory to quantitatively interpret probes. However, by placing a small floating probe (pin) in front of a larger probe (plate) it appears possible to extract the variation of the plate sheath potential drop with plate current experimentally [5] and hence side-step this whole problem.

In the JET Mark I divertor 4 probes were connected permanently to a 1MHz data acquisition system. In Mark II the system will more flexible with capability of switching up to 16 probes into the fast data acquisition system under remote control.

7. Conclusions

Previous experience at JET, which is consistent with that of all other large tokamaks, is that fixed probe systems are unreliable and labour intensive to operate and maintain. Major technical advances have been made at JET in the areas of probe design, electronics and control which dramatically change this situation. The new pumped divertor probe system has operated reliably for over a year of JET operation with relatively low maintenance despite an order of magnitude increase in the number of probes installed. An intelligent control system ensures that fault conditions are automatically dealt with and the maximum volume of useful data is assured. The success of the JET probe system has had a very strong influence on the current probe design for ITER and led to greater confidence that fixed probes can be designed which will last long enough to be relevant to ITER's needs.

A similar fixed probe system is planned for the Mark II divertor but with the addition of "pop-up" probe drives which will be used to insert pin-plate probes into the divertor plasma. These probes offer the prospect of a technical solution to the problem of plasma resistivity which can seriously affect the interpretation of Langmuir probe data.

Acknowledgement

The new JET probe system was only possible with the professional engineering expertise of: H.E.Clarke, K.Fullard, E.McCarron, C.Hogben, G.Neill and X.Tellier.

References

[1] R.D.Monk et al., this proceedings.
[2] G.F.Matthews, Plas. Phys. Cont. Fus. **36** (1994) 1595-1628
[3] Hibbit, Karlsson and Sorensen Inc., Providence, RI. *ABAQUS Users Manual, version 4.6,* 1987
[4] H.Guo et al., 22^{2n} Conf. on Cont. Fus. and Plas. Phys., Bournemouth, 1995
[5] P.C.Stangeby, JET preprint number JET-P(95)21
[6] K.Gunther, 22^{2n} Conf. on Cont. Fus. and Plas. Phys., Bournemouth, 1995

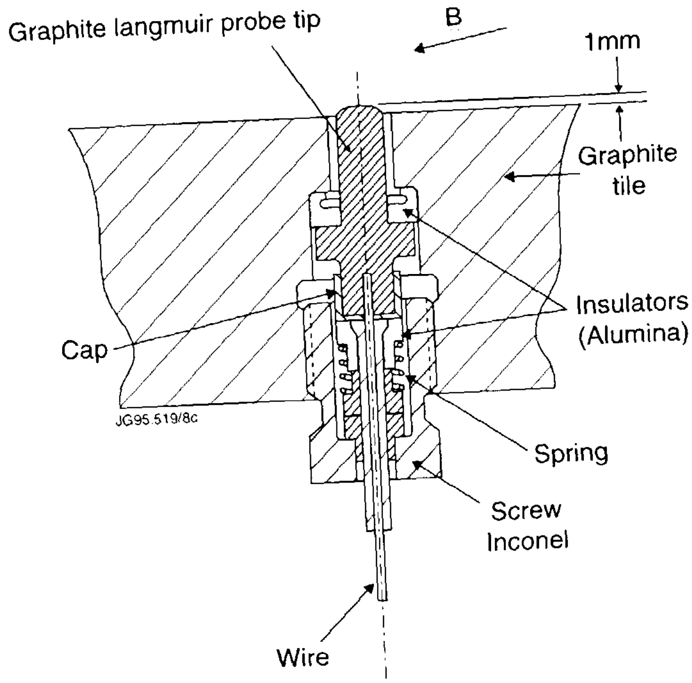

Figure 1: Original JET probe design used until 1992.

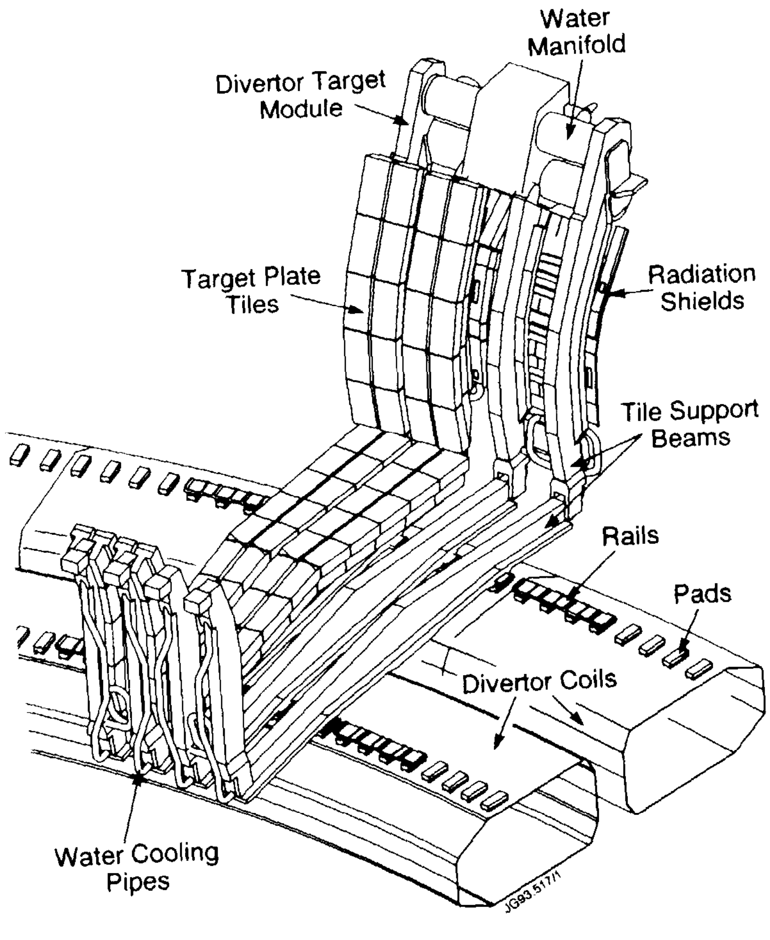

Figure 2: Mark I pumped divertor structure with some tiles removed to show support beams.

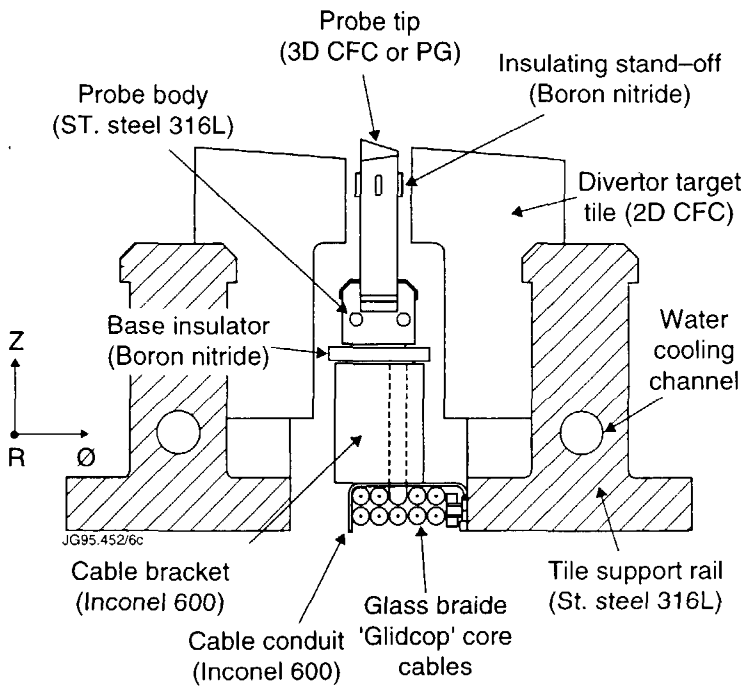

Figure 3: Mark I divertor probe assembly.

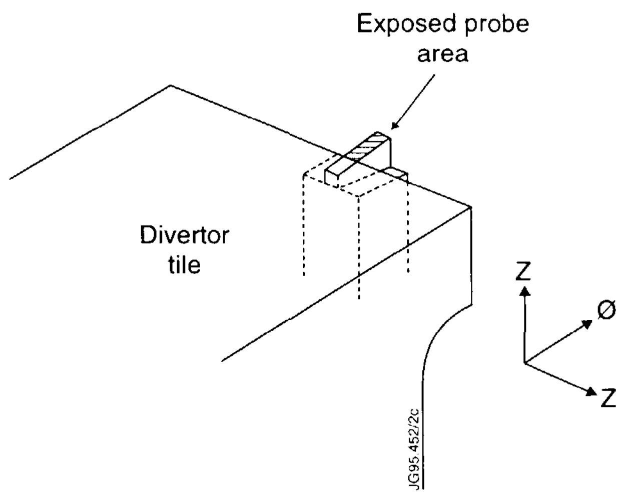

Figure 4: The relationship between the probe tip and tile.

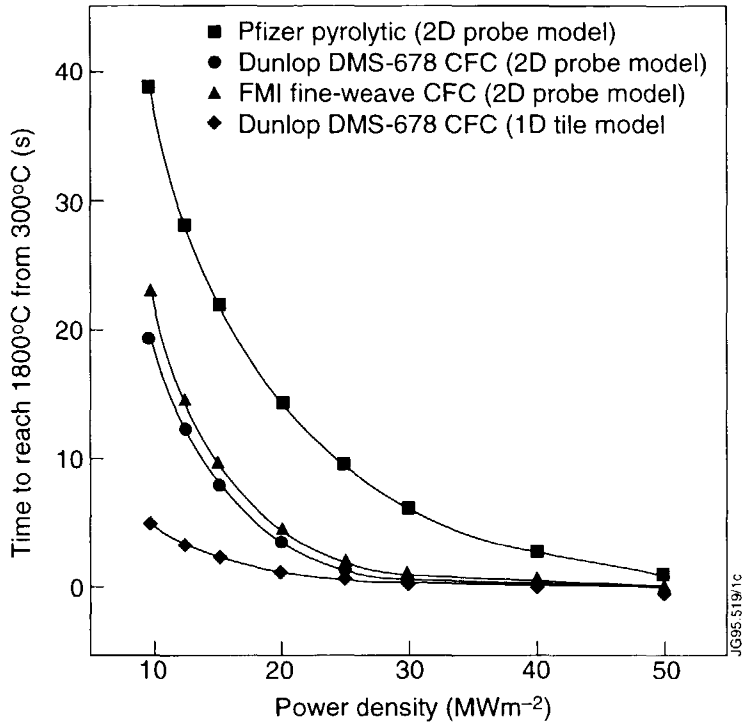

Figure 5: Finite element calculations for the time taken for the probe tip surface to reach sublimation temperature for a range of materials.

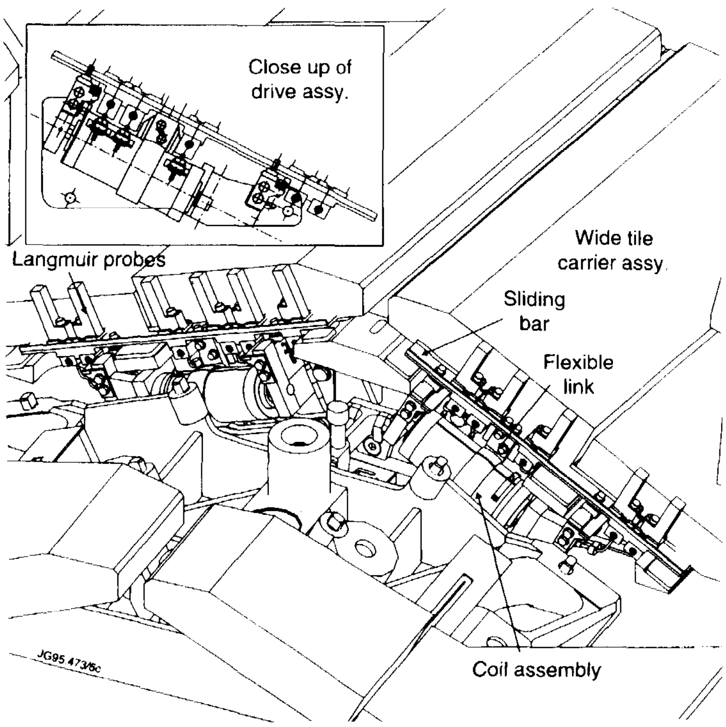

Figure 6: Mark II divertor structure and location of "pop-up" probe systems.

The JET Reciprocating Probe Systems - Performance and Data Analysis

S. J. Davies, K. Erents[1], H. Y. Guo[2], A. Loarte, G. F. Matthews, K. McCormick[3] and R. D. Monk[4]

JET Joint Undertaking, Abingdon, Oxon., OX14 3EA, UK.
[1] UKAEA Fusion, Culham, Abingdon, Oxon., OX14 3DB, UK.
[2] INRS-Energie et Materiaux, Université du Quebec, Canada.
[3] Max-Planck-Institut für Plasmaphysik, EURATOM Association, 85748 Garching, Germany.
[4] Department of Physics, Royal Holloway College, University of London, Surrey, UK.

Abstract The JET reciprocating probe systems are described. This paper will also cover determination of separatrix position using the pressure balance method. Use of floating potential to indicate separatrix location is shown to be incorrect. Other topics covered are comparison of upstream profiles with both lithium beam and 'onion-skin' modelling, experience with triple-probe operation for ELM studies and the development of a boron-nitride probe head.

1. Introduction

The JET reciprocating probe systems were used extensively during the MkI divertor experimental campaign to measure upstream scrape-off layer (SOL) parameters and fall-off lengths. This paper is concerned with a description and an outline of the data analysis performed on the data from these systems. Following a description of the reciprocating systems, the method for determining the separatrix position using pressure balance will be given. Comparison of upstream profiles with both lithium beam and 'onion-skin' modelling will be presented as well as experience with triple probe operation particularly for ELM studies. Finally the development and use of boron-nitride probe heads will be described.

2. Details of reciprocating probe systems

JET has two reciprocating probe systems situated at the top of the vessel (Figure 1) in Octants 1 and 5. Reciprocation strokes up to 250mm long can be programmed to occur up to eight times during a pulse (four per system). Each stroke typically takes ≤1 second. Langmuir probe heads consist of six Langmuir elements (three on the ion-drift side and three on the electron drift side) orientated perpendicular to the magnetic field lines. Each probe tip is embedded within an alcove of the probe body. This probe arrangement makes it possible to deduce the plasma flow direction and Mach number. The probe body used to be made from 3-D weave CFC carbon which has excellent thermal conductivity, thermal shock resistance and strength. More recently a boron-nitride probe body has been developed and this is described further in Section 6.

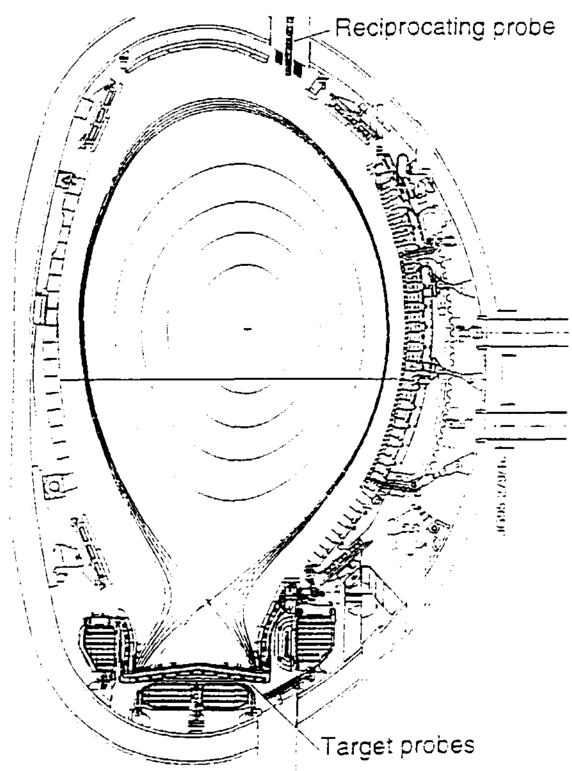

Figure 1 : Relative location of reciprocating and fixed probes in JET.

One of the systems has also been used with a Retarding Field Analyser (RFA) [1] and Collector probe heads. It is possible to exchange probe heads overnight using a specially designed exchange chamber. The collector probe utilises the rotary drive facility so that both time-resolved and time-integrated sample exposures can be performed.

3. Determination of separatrix position

Use of the reciprocating probes at JET requires first a reference pulse from which the separatrix position given by the equilibrium codes EFIT and XLOC can be deduced. Unfortunately the separatrix position given by these codes rarely agreed [2] and a more practical determination of the separatrix position was achieved from an assessment of the ion-saturation signal.

For the analysis of data and comparison of the upstream parameters with the target data a more robust procedure for the separatrix position was required. Pressure balance as defined in the two-point model [3] with the assumption of $T_e = T_i$, i.e.

$$0.5\, n_e^{Up}\, T_e^{\ Up} = n_e^{tgt}\, T_e^{tgt} \tag{1}$$

was found to be the most reliable method although it is only valid for sheath limited ($T_e^{Up} \approx T_e^{tgt}$) and high recycling ($\nabla T_e$ large) plasmas but not during detachment. The premise is that the upstream separatrix position does not change with the onset of detachment.

The pressure balance method involves defining the separatrix position at the target as the peak in the ion-flux which, for the MkI target probes, gives the separatrix position to an accuracy of 2mm. The upstream pressure profile is then shifted until the pressures match as shown, for example, in Figure 2. Also shown are the density, temperature and floating potential profiles. Note the rapid decrease in the floating potential close to the separatrix.

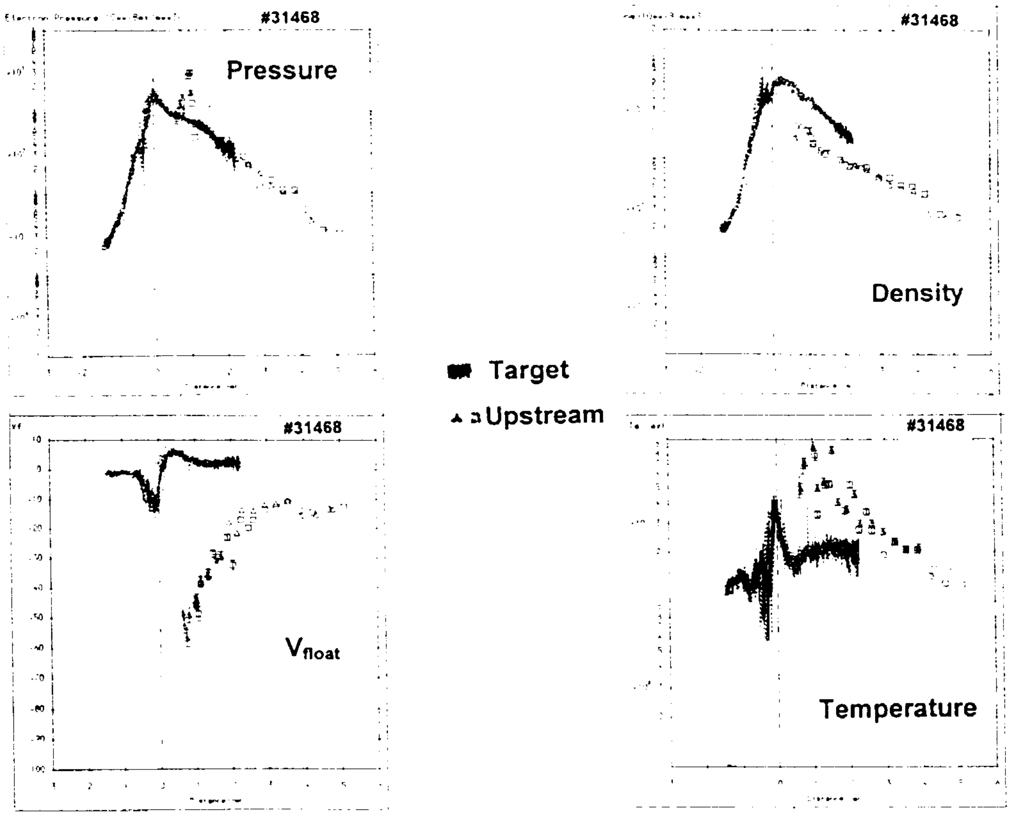

Figure 2 : Upstream and target pressure balance with corresponding floating potential, electron density and temperature profiles.

The rapid decrease in the floating potential has been used [4] as an indicator of separatrix position and Figure 2 does appear to indicate that $\delta V_f/\delta r \rightarrow \infty$ also gives the separatrix position. This is not strictly true as the example in Figure 3 indicates. The pressure balance shows that the reciprocating probe has gone ~0.5 midplane cm past the separatrix in this instance. The corresponding temperature and floating potential profiles both plotted on linear axes are also given showing that $V_f \propto -T_e$.

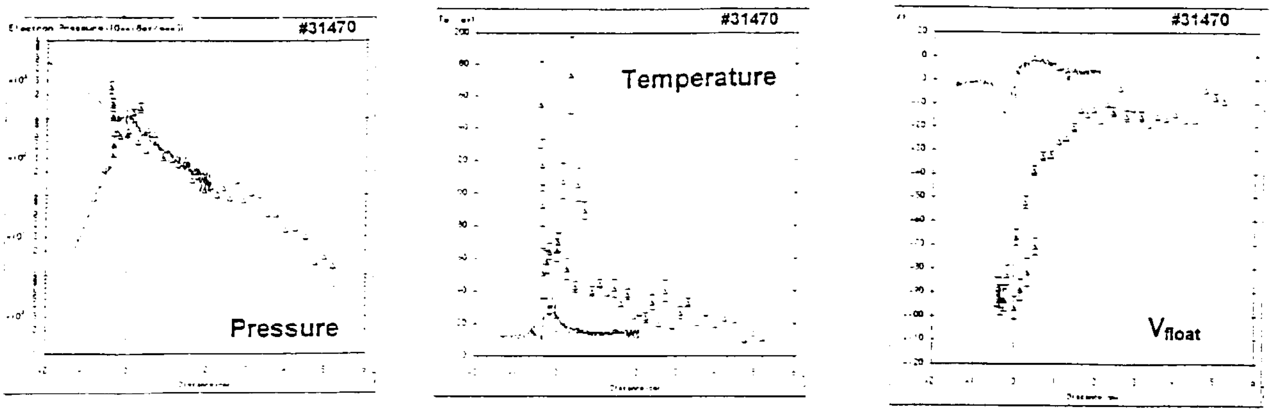

Figure 3 : Upstream and target pressure, temperature and floating potential profiles clearly showing $V_f\ \alpha\ -T_e$

This may be understood through

$$\text{Electric field, } Er = -\frac{\delta Vf}{\delta r} - 2.5\frac{\delta Te}{\delta r} \qquad (2)$$

where it has been observed at JET that the electric field calculated from reciprocating probe measurements is essentially zero in ohmic and L-mode pulses; thus $V_f\ \alpha\ -T_e$. The electric field has been used [5] elsewhere to investigate the L-H transition and is not relevant for these data. Calculation of the electric field at the separatrix is subject to large errors owing to the large error in electron temperature as a result of a saturated current signal and, in some instances, because there is a significant cooling effect on the local plasma caused by sublimation of part of the probe. This is seen as a hysteresis in the temperature and floating potential profiles. The corruption of data by this cooling is avoided by using only data on the inward stroke of the reciprocation. Smaller probe areas will be used in the next experimental campaign to alleviate the saturation of the current signal.

4. Comparison of upstream profiles with lithium beam diagnostic and 'onion-skin' modelling

JET also has a lithium beam diagnostic situated at the top of the vessel and at the same major radius as the reciprocating probes [6]. Over a series of pulses both the reciprocating probe and lithium beam diagnostic recorded density profiles at the same time and an example of the excellent agreement between the two profiles, plotted as a function of distance at the probe/lithium beam location, is shown in Figure 4a. The profiles have been shifted relative to each other by 2cm (~0.8 midplane cm) which is within the accuracy of the absolute position of these diagnostics.

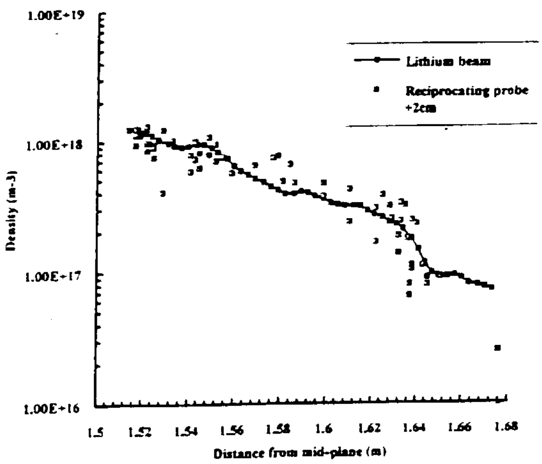

'Onion-skin' [7] modelling which calculates the upstream density and temperature profiles using the measured target profiles as input was performed on several L-mode discharges with (2 - 8.5)MW neutral beam injected power. The calculated upstream profiles may then be compared with the measured profiles as illustrated in Figure 4b,c for 2MW and 4.9MW neutral beam injected power. There is good agreement between the measured and calculated upstream density and

Radial Profiles of Upstream Density

Shots: 31462,31468

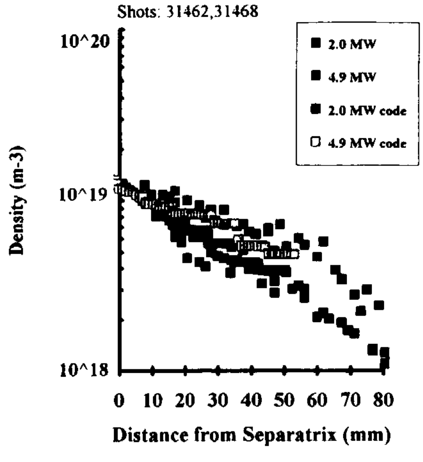

temperature profiles. The larger scatter in the temperature profiles is a common observation of reciprocating probe measurements and is understood to be attributed to fluctuations. It is intended to investigate this further in the MkIIa experimental campaign using the triple probe arrangement in conjunction with fast sampling ADCs.

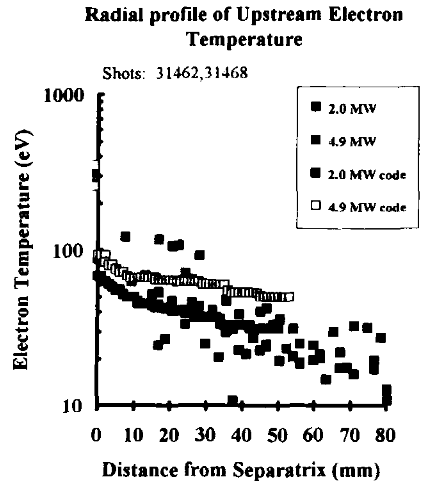

Figure 4 : Comparison of upstream profiles with (a) Li beam diagnostic and (b, c) 'onion-skin' modelling.

5. Triple probe operation

The arrangement of probe tips allows either single or triple probe modes of operation as used in the target Langmuir probes [8]. The advantage of triple probe operation is that measurements of, for example, ion-flux and electron temperature can be made at a faster sampling rate (10kHz for the data presented here) useful for the study of ELMs. Initially a comparison of single and triple probe modes of operation was performed to identify any differences. Data for the ion- and electron- drift sides of the probe were operated in single(triple) then triple(single) probe mode in two identical pulses. Generally good agreement was obtained between the ion-flux profiles but there appears to be a problem with the electron temperature profiles owing to a significant leakage current which results in low or zero electron temperatures in some cases. The cause of this leakage current is currently under investigation and the problem will be resolved in time for the MkIIa divertor operations.

Triple probe measurements during ELMy H-modes have been performed as illustrated in Figure 5. This shows the ion-flux as recorded by the target and reciprocating probes along with the D_α signal. The probe current as measured by the reciprocating probe saturates during an ELM even though the underlying ion-flux signal is low as a result of being ~3 midplane cm away from the separatrix. With smaller probe areas and a boron-nitride probe body ELM behaviour up to the separatrix will be investigated in the MkIIa divertor campaign. It is still possible to determine the underlying SOL width for these ELMy H-mode pulses [9].

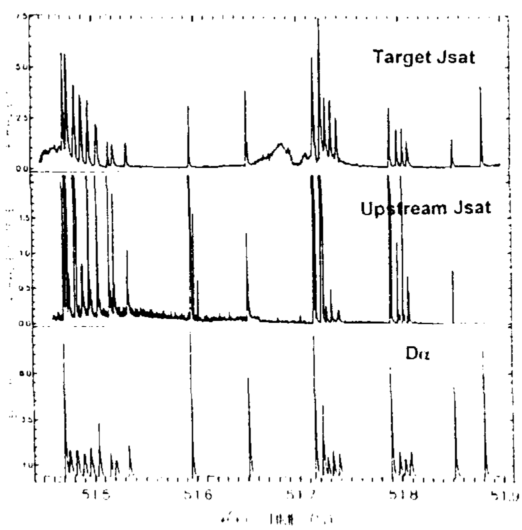

Figure 5 : Target and upstream ion-flux profiles and D_α signal for ELMy H-mode pulse.

6. Development of boron-nitride probe heads

Following the breakage of a carbon CFC probe head during plasma operations it was decided to develop a boron-nitride probe which owing to its excellent insulating properties (volume resistivity $>10^{14}$ Ωm compared to $\sim 1.5\times10^{-5}$ Ωm for CFC graphite) would not experience significant JxB forces as happened for the CFC probe. Before this probe development is described further a synopsis of the events which caused the breakage of the CFC probe is given.

A Vertical Displacement Event (VDE) occurred during a reciprocation into a 10MW neutral beam injected H-mode plasma resulting in the rupture of one of the CFC probes. The other system reciprocating at the same time and to the same location was undamaged. The sequence of events [10] appears to have been started by a Giant ELM which caused the Fast Radial Field Amplifier (FRFA), which controls the vertical position of the plasma, to trip after 5ms. It is not clear whether the Giant ELM occurred as a result of an influx of dislodged graphite caused by the movement of the reciprocating probe.

The electrical isolation of the probe failed owing to the proximity of plasma/radiation/gas. The floating potential at the time was ~-150V as measured by the other reciprocating probe. When the probe broke it was probably immersed up to 70cm in the halo current and confined part of the plasma 34ms after the VDE. The current through the probe at this time, from mushroom current measurements, was estimated to be ≥ (2-4)kA. A 2kA current would produce a 36MPa bending stress on the CFC which is very much less than its failure bending stress which was calculated to be 400MPa. The current required to produce this bending stress is 22.5kA (~1% of total plasma current in this pulse). The broken probe landed in the outer corner of the MkI divertor and did not prevent further plasma operations as regular inspection revealed that it did not move. There was no impurity contamination from the probe either as the only materials used in the probe head were carbon and boron-nitride.

The Neutral Beam test bed facility at JET was used to ascertain the thermal performance of a boron-nitride probe. Several tests were undertaken [11] and Figure 6 shows the temperature behaviour for two of these. In Figure 6a the probe was exposed to 40MW/m^2 for 50ms separated by a one second interval to simulate the reciprocation cycle in plasma. This was repeated 300 times after which there was no observable damage to the probe. The temperature of the probe went up to ~2000°C which was specified to be the sublimation temperature for boron-nitride but no sublimation was observed. In Figure 6b the probe was exposed to 40MW/m^2 for 220ms and the extrapolated peak temperature was ~3400°C. Only at this power density was there an observable darkening of the probe body and it is thought that the boron and nitrogen dissociated at these high temperatures leaving the boron on the surface. The probe was also exposed to 10MW/m^2 for 2s and again no damage was observed.

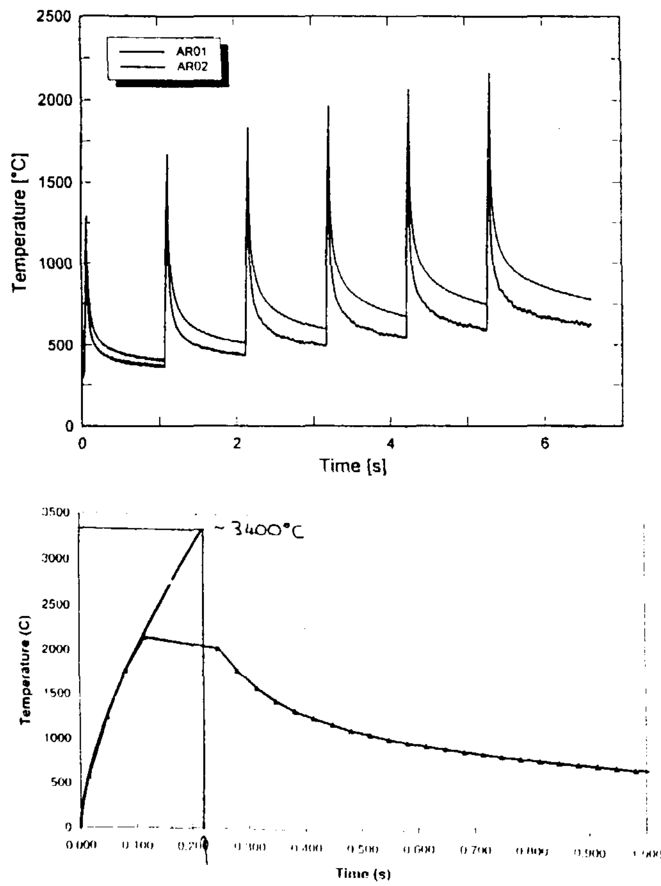

Figure 6 : Temperature excursions of boron-nitride probe for (a) 40MW/m^2 on, 1s off and (b) 40MW/m^2 for 220ms.

The final test was to use a boron-nitride probe in plasma at the end of the MkI divertor experimental campaign when a disruption was deliberately caused at the same time as the reciprocation of the probe. No damage to the probe occurred. It is intended to continue using boron-nitride probes in the MkIIa experimental campaign.

7. Conclusions

JET's reciprocating probe systems were extensively used during the MkI divertor experimental campaign providing an abundance of upstream SOL measurements essential for model validation. For the MkIIa experimental campaign one of the systems is to be upgraded so as to have a stroke length of up to 400mm. A Plasma Ion Mass spectrometer (PIMS) probe head is also currently being designed for use alongside the RFA and Collector probe heads.

The most reliable method for the determination of the separatrix position is using pressure balance. Use of the floating potential is not a reliable method as its profile simply mirrors the increase in electron temperature. Good agreement between the upstream lithium beam and reciprocating probe density profiles has been obtained as well as with 'onion-skin' modelling work. A boron-nitride probe has been successfully developed and tested and will be used in the MkIIa experimental campaign to further investigations into ELMy and ELM-free H-mode SOL physics.

8. References

[1] Guo, H. Y. et al., this workshop
[2] Erents, K. et al., Proc. 22nd EPS, Bournemouth (1995)
[3] Keilhacker, M. Et al., Physica Scripta **T2/2**, 443 (1982)
[4] see, for example, Zushi, H. Et al., Proc. 22nd EPS, Bournemouth (1995)
[5] Gohil, P. et al., Proc. 21st EPS, Montpellier (1994)
[6] Breger, P. et al. Proc. 22nd EPS, Bournemouth (1995)
[7] Monk, R. D. et al., J. Nucl. Mat., **220-222**, 612 (1995)
[8] Matthews, G. F. et al., this workshop
[9] Erents, K., UKAEA Fusion Internal Report F/PH/KE/A10/3(95)
[10] P. Noll, personal communication
[11] Godden, D. J. et al., JET-IR(95)01

9. Acknowledgements

The authors would like to acknowledge D. J. Campbell and Task Force D for their support of the reciprocating probe systems. They also acknowledge the expertise of C. Hogben, G. Kaveney, G. Neill, J. Vince and D. Wilson whose skill and commitment have made such measurements possible.

Divertor Langmuir Probe Measurements in JET

R.D. Monk† A. Loarte, A. Chankin, S. Clement, S.J. Davies
K. Günther, H.Y. Guo‡ J. Lingertat, C.F. Maggi
G.F. Matthews , M.F. Stamp and A. Tabasso§

JET Joint Undertaking, Abingdon, Oxfordshire, OX14 3EA.
† Royal Holloway College, University of London, Surrey, TW20 OEX.
‡ INRS-Energie et Materiaux, University du Quebéc, Canada.
§ Imperial College of Science, Technology and Medicine, London, SW7 2BZ, UK.

Abstract

In this paper, results from the array of fixed Langmuir probes in the JET Mk. I divertor are presented. During low density discharges there is good agreement between single and triple probes. At higher density, near the onset of divertor detachment, very low values of the electron to ion saturation current (even < 1) are observed which results in an overestimation of the electron temperature, particularly by the triple probe. Alternative methods of probe interpretation are applied and comparisons carried out with independent measurements. The consistency of probe measurements during H-mode discharges are also briefly discussed.

1 Introduction

Langmuir probes remain one of the most commonly applied diagnostics for the study of the scrape-off layer plasma in tokamaks. For the recent Mk. I pumped divertor phase of JET [1], an array of 117 Langmuir probes, which can be configured as single or triple probes, were installed in the target plates. Triple probes have the advantage of providing a continuous measurement of plasma parameters and are essential for studying fast phenomena such as ELMs which normally corrupt the characteristics of single probes. In addition, with sweeping of the divertor strike points across the target, it has been possible to measure high resolution profiles across the divertor plasma and identify features not previously resolved by discreet single probe measurements. This paper describes the analysis and interpretation of data from the divertor probe array and highlights conditions under which of the conventional methods of probe interpretation appears to be invalid. After a brief description of the data analysis procedure, probe measurements under ohmic, L-mode and H-mode conditions are described. The technical performance of the probe system is described in the companion paper by Matthews et al. [2].

2 Data Analysis Procedure

Due to the wide variation in strike point positions possible with the new in-vessel divertor coils, 149 fixed probes were installed in the target plates, of which 117 can be separately configured as triple or single probes. After every discharge the raw data is archived to the IBM3090 mainframe computer where analysis software is used to convert the raw signals into physical quantities and store in a format which is compatible with the standard JET data display software. For the triple probes the data analysis procedure is relatively simple [3] and the plasma parameters are calculated at the data acquisition rate of $5kHz$. In the case of the single probes, the bias waveform is typically ramped from -100 to $+25V$ over a $5ms$ period to provide 25 points per current-voltage (I-V) characteristic. With longer ramp periods the characteristics are distorted due to the movement of the strike points duing $4Hz$ sweeping. The single probe characteristics are fitted with the simple exponential formula

$$I = I_{sat}(1 - \exp[e(V - V_f)/kT_e])$$

where I_{sat} is the ion saturation current, V_f the floating voltage and T_e the electron temperature. The fitting is carried out using the Gridsearch [4] method for non-linear least squares fitting. Previous experience of scrape-off layer probe measurements at JET has shown that fitting the I-V characteristic beyond the floating voltage tends to overestimate the T_e due to deviations from the simple exponential [5]. However, with only 25 points per I-V characteristic, if too few points are included near V_f then statistical errors can dominate and make the fitting procedure problematic. In practice, the compromise solution is to carry out a series of fittings each including successively fewer points beyond V_f and choose the fit which provides the lowest T_e whilst not introducing large statistical errors.

Following the virtual double probe approach introduced by Günther [6], the asymmetric double probe fit has recently been applied to analyse the probe characteristics. This method has the advantage of fitting the whole characteristic and consequently reducing the statistical errors. However, to enable rapid convergence of the least squares fitting, the characteristic is initially fitted with the single exponential formula using the procedure described above to anchor the I_{sat} and V_f values. The influence of using the asymmetric double probe formula on the derived divertor plasma parameters is described in the following section.

To reduce the average power density on the divertor target plates, the strike points are routinely swept at $4Hz$. For divertor probes that are crossed by the separatrix, the fast boundary reconstruction code XLOC [7] is used to determine the separatrix location in relation to the probes and convert the time vector of the probe signal into a series of radial profiles every $125ms$. It is then possible to integrate over the triple probe profiles to conveniently calculate the particle and power fluxes to the divertor without the requirement to fit decay lengths. One such example is shown in fig. 1 for an ohmic, low density discharge during which the outer strike point is slowly swept across triple and single probes. These high resolution profiles have allowed the clear identification of narrow features of current flow, multiple strike zones and non-exponential profiles that would be difficult to resolve with only single probes and unswept discharges.

Figure 1 : Profiles of ion saturation current (I_{sat}), electron temperature (T_e) and electron density (n_e) derived from triple and single probe measurements as the separatrix is swept across the outer divertor target.

3 Ohmic Discharges

One of the basic measurement of Langmuir probes is the ion saturation current, I_{sat}, whereby a large negative bias repels all the electrons. Due to the compound angle of typically $> 15°$ between the field lines and probe tip, non-saturation of the ion current has not been observed. Since the ion flux to the divertor target is generally dominated by the recycled neutrals, comparisons can be carried out with the divertor D_α photon flux after choosing a suitable value for the number of ionisations per photon. From Johnson and Hinnov [8], with typical ohmic divertor parameters of $10 - 20eV$ and $10^{19}m^{-3}$, the factor is reasonably constant and taken to be 20. For pulse #34314, the integrated ion flux of $8.7 \times 10^{22}s^{-1}$ lies between the result calculated from visible spectroscopy ($5.9 \times 10^{22}s^{-1}$) and the flux camera ($15.8 \times 10^{22}s^{-1}$) diagnostics. Similar levels of agreement can be obtained by comparing with the flux derived from the neutral pressure gauges in the divertor.

To study the influence of main plasma density on the divertor parameters derived from the probes, the ohmic density ramp discharge #31627 is selected. One can see from fig. 2 that as the density increases the profiles of the ion saturation current peak and then begin to fall at $\bar{n}_e > 3 \times 10^{19}m^{-2}$ signifying the onset of divertor detachment [9] until the density limit occurs at 57.6s. Profiles across the outer divertor target are selected at three different times indicated by the dashed line; low recycling at 54.5s, high recycling at 55.7s and detachment at 56.9s. Fig. 3 shows the radial profiles of I_{sat} and T_e where the solid line shows the triple probe measurements and the two sets of points represent the single probe data using the simple exponential and asymmetric double probe formulae. During the low recycling phase there is good agreement between all three T_e profiles with around $15 - 20eV$ at the separatrix. However, for the high recycling phase the triple probe measures $70eV$ at the separatrix and the double probe measures around $7eV$ - approximately half that of the single probe. Finally, during divertor detachment the different T_e measurements are more closely grouped together with the asymmetric double probe measuring

$2-3eV$. It is useful to compare these measurements with the profiles of the electron to ion saturation current ratio (I_{sat}^{-}/I_{sat}^{+}) shown in fig. 4 and derived from the asymmetric double probe fitting. During the low recycling phase the ratio lies between 8-15 in the SOL and the characteristics closely resemble that of a single probe. In the high recycling phase, where the triple probe measures an unphysical T_e of $70eV$, the ratio approaches unity and the slight asymmetry of the probe tip areas is sufficient to drive the electron collecting element of the triple probe beyond the knee of the characteristic. Simulations of this discharge carried out with the EDGE2D code [10] predict outer divertor T_e separatrix values of $12-20eV$ (low recycling), $4-7eV$ (high recycling) and $1-2eV$ (detachment). It would appear that the asymmetric double probe matches these values more closely than the conventional exponential fit. However, on the inner divertor plate the functional form of the characteristics is not well reproduced by the asymmetric double probe model and the current appears to increase linearly beyond the floating voltage with $T_e = 5-10eV$ during detachment. Recently, the effect of plasma resisitivity on probe interpretation in cold and dense divertor plasmas has been considered by Günther [11]. Applying the theory to the outer T_e profiles of #31627 would appear to overestimate the effect and results in $2-3eV$ at the seperatrix for all three phases of the discharge. This may be related to the assumption of slab geometry in the model which underestimates the area of the flux tube through which the cross-field current may be drawn.

Figure 2 : Plasma parameters for the ohmic discharge #31627 in which the main plasma density is increased up to the limit at 57.6s.

Figure 3 : Radial profile of the ion saturation current and electron temperature for the three phases of discharge #31627.

Figure 4 : Profile of the electron to ion saturation current ratio derived from the asymmetric double probe fits.

4 L-Mode Discharges

Similar trends are observed during L-mode discharges to the ohmic cases described above although fig. 5 shows an extreme example that has I-V characteristics with $I_{sat}^{-}/I_{sat}^{+} \sim 0.5$ at high density and with $4MW$ of auxiliary heating. Since the target tile temperature during L-mode discharges is often above the detection threshold of the infra-red thermography, it is possible to compare the deposited power with that from the divertor probes. Considering two discharges with $4MW$ heating and line averaged density of $3\times10^{19}m^{-2}$, #31591 has the $\mathbf{B}\times\nabla\mathbf{B}$ drift directed towards the target and #31485 away. In the case of #31591 the inner divertor is approaching detachment with over an order of magnitude larger level of D_α photon flux compared to #31485. Calculating the deposited power from the probes (including the contribution from surface recombination) gives $4.2MW$ for #31591 compared with $2.9MW$ and $3.9MW$ compared with $3.7MW$ for #31485. Clearly, the power balance is much improved in discharges with lower levels of recycling.

By using spectroscopic line ratios that are sensitive to the electron temperature it is possible to carry out a more direct comparison with the probe results. For discharge #35723 with $3MW$ of additional heating, the main plasma density is increased up to the density limit at $9.5\times10^{19}m^{-2}$. During this period the inner divertor is viewed by the VUV spectrometer which is T_e sensitive in CII for the ratio $90.41/133.53nm$ while the outer is diagnosed by the thermal helium beam and periscope spectrometer sensitive to T_e for the ratio $728/706nm$ and n_e with $668/728nm$ [13]. Fig. 6 shows the variation in inner and outer I_{sat} and T_e with the corresponding points derived from the spectroscopic line ratios. It should be noted that the VUV spectrometer was not directly viewing the strike zone and so the measurements should only be regarded as an upper limit.

Figure 5 : Example from the high density L-mode discharge #31504 in which I-V characteristics with an electron to ion saturation current ratio of less than unity are measured.

Figure 6 : Comparison of single probe electron temperatures with line ratios derived from the VUV spectrometer on the inner plate and the thermal helium beam on the outer.

5 H-mode Discharges

In the pumped divertor configuration of JET the H-mode discharges are naturally ELMy which previously corrupted the characteristics of single probes. Using the continuous measurements afforded by new triple probes, it has been possible to measure the divertor parameters during discharges with regular ELMs. During each sweep on can assign an effective half-width to the profile through the envelope defined by the peaks of the ELMs. By assuming an average ELM frequency, the total power and particle fluxes to the divertor can be calculated and preliminary results are encouraging.

During hot ion H-mode discharges the divertor parameters have also been measured using the probes. Typical divertor parameters under these conditions are $T_e = 40 - 60eV$ with $n_e = 5 - 9 \times 10^{18}m^{-3}$ and good agreement with the D_α photon fluxes are obtained. However, the power depositied on the plate is significantly underestimated (compare $1.1MW$ calculated from the probes to $P_{IN} - dW/dt - P_{rad} = 7.63MW$ for pulse #33094). It is likely that the assumptions of $T_i = T_e$ [14] and neglect of the s.e.e. yield used in the calculation of the sheath power transmission factor are not valid under these conditions.

6 Conclusions

Divertor probe measurements have made a significant contribution to the analysis of experiments carried out with the JET Mk. I pumped divertor. In particular, the combination of triple probe measurements with strike point sweeping have enabled the measurement of high resolution divertor profiles not previously possible. As a basic parameter, the ion saturation current is consistent with measurements of divertor D_α and neutral fluxes. At low density the single and triple probes agree well but diverge at higher density due to low values of the electron to ion saturation current ratio (< 1 in some cases). On the outer target, application of the asymmetric double probe formula improves the consistency of the results with respect to code calculations but the interpretation of the inner plate probes remains to be addressed. In the next experimental campaign it is planned that pin/plate probes will be used and these will help to experimentally address some of the probe interpretation issues encountered during high density discharges. The triple probes have been used to study divertor plasma parameters during ELMs and futher analysis is underway. During hot-ion H-modes the power flowing to the divertor target is underestimated and attributed to $T_i > T_e$ and uncertainty in the s.e.e. yield.

7 Acknowledgements

The authors would like to acknowledge the Divertor Physics Task Force and Topic Group for their support of this work. RDM acknowledges financial support from the Engineering and Physical Sciences Research Council.

References

[1] Bertolini, E. and the JET Team, *Fusion Engineering and Design* **30** (1995) 53

[2] Matthews, G.F. , Davies, S.J. and Monk, R.D., *these proceedings.*

[3] Chen, S.-L. and Sekiguchi, T., *Jour. App. Phys.* **36** (1965) 2363

[4] Bevington, P.R., Data Reduction and Error Analysis for the Physical Sciences", McGraw Hill (1969) 212.

[5] Tagle, J.A., Stangeby, P.C. and Erents, S.K., *Plasma. Phys. and Cont. Fusion* **29** (1987) 297.

[6] Günther, K., Herrmann, A., Laux, M., et al., *J. Nucl. Mater.*, **176-177** (1990) 236.

[7] O'Brien, D.P., Ellis, J.J, Lingertat, J., *Nucl. Fusion* **33** (1993) 467.

[8] Johnson, L.C. and Hinnov, E., *J. Quant. Spectro. Radiat. Transfer* **13** (1973) 333.

[9] Monk, R.D., Campbell, D.J., Clement, S., et al., *Proc. 22nd EPS Conf.*, Bournemouth (1995).

[10] Taroni, A., Corrigan, G., Horton, L.D., et al., *Proc. 22nd EPS Conf.*, Bournemouth (1995).

[11] Günther, K., *Proc. 22nd EPS Conf.*, Bournemouth (1995).

[12] Chankin, A.V., Campbell, D.J, Clement, S., et al., *Proc. 22nd EPS Conf.*, Bournemouth (1995).

[13] Schweer, B., Mank, G., Pospieszczyk, A., *J. Nucl. Mater.* **196-198** (1992) 174.

[14] Guo, H., et al., *these proceedings*.

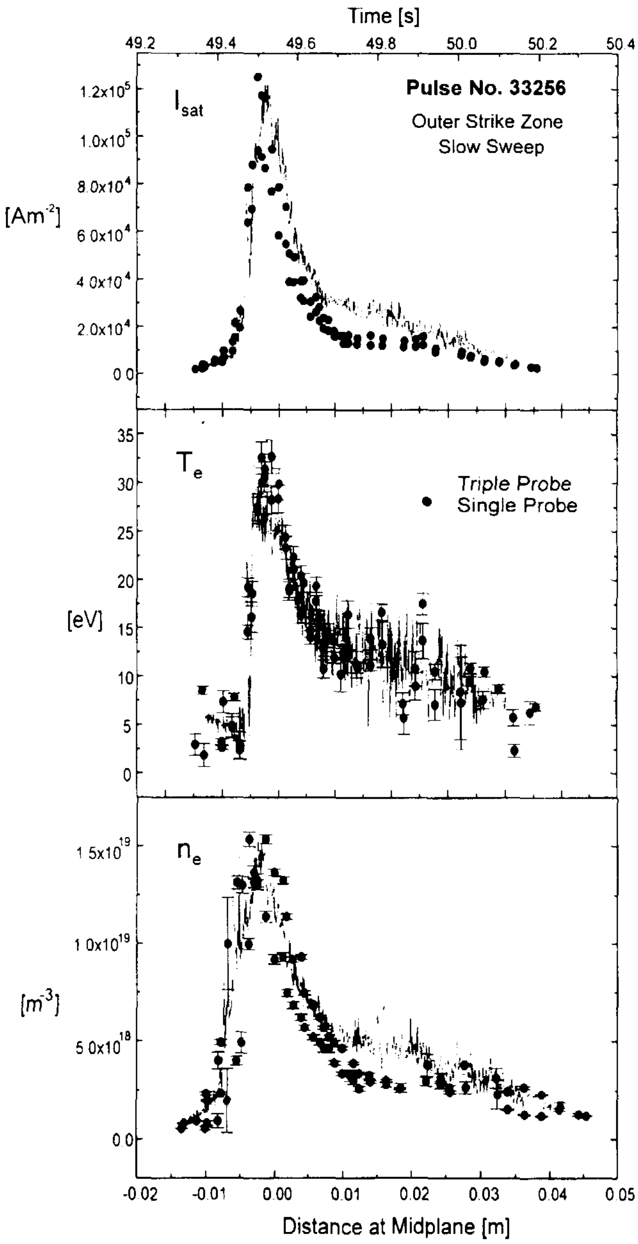

Time [s]
49.2
49.4
49.6
49.8
50.0
50.2
50.4
Pulse No. 33256
Outer Strike Zone
Slow Sweep
I_sat
[Am^-2]
1.2x10^5
1.0x10^5
8.0x10^4
6.0x10^4
4.0x10^4
2.0x10^4
0.0
T_e
Triple Probe
Single Probe
[eV]
35
30
25
20
15
10
5
0
n_e
[m^-3]
1.5x10^19
1.0x10^19
5.0x10^18
0.0
-0.02
-0.01
0.00
0.01
0.02
0.03
0.04
0.05
Distance at Midplane [m]

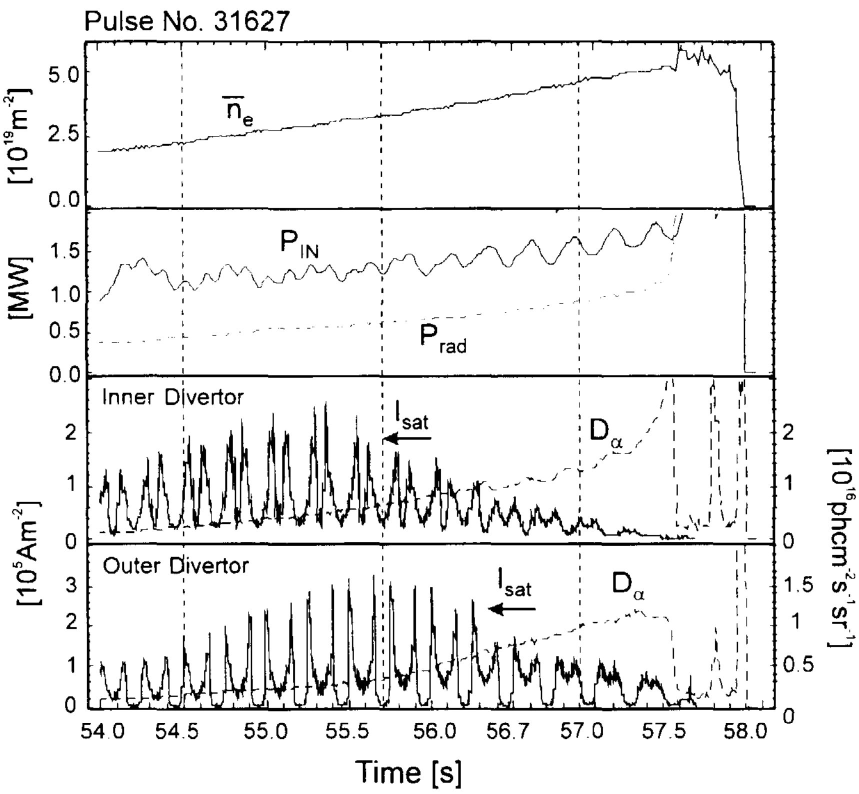
Pulse No. 31627
[10^{19}m^{-2}]
$\bar{n}_e$
5.0
2.5
0.0
[MW]
P_{IN}
P_{rad}
1.5
1.0
0.5
0.0
Inner Divertor
I_{sat}
D_α
Outer Divertor
[10^5Am^{-2}]
[10^{16}phcm^{-2}s^{-1}sr^{-1}]
Time [s]
54.0
54.5
55.0
55.5
56.0
56.7
57.0
57.5
58.0

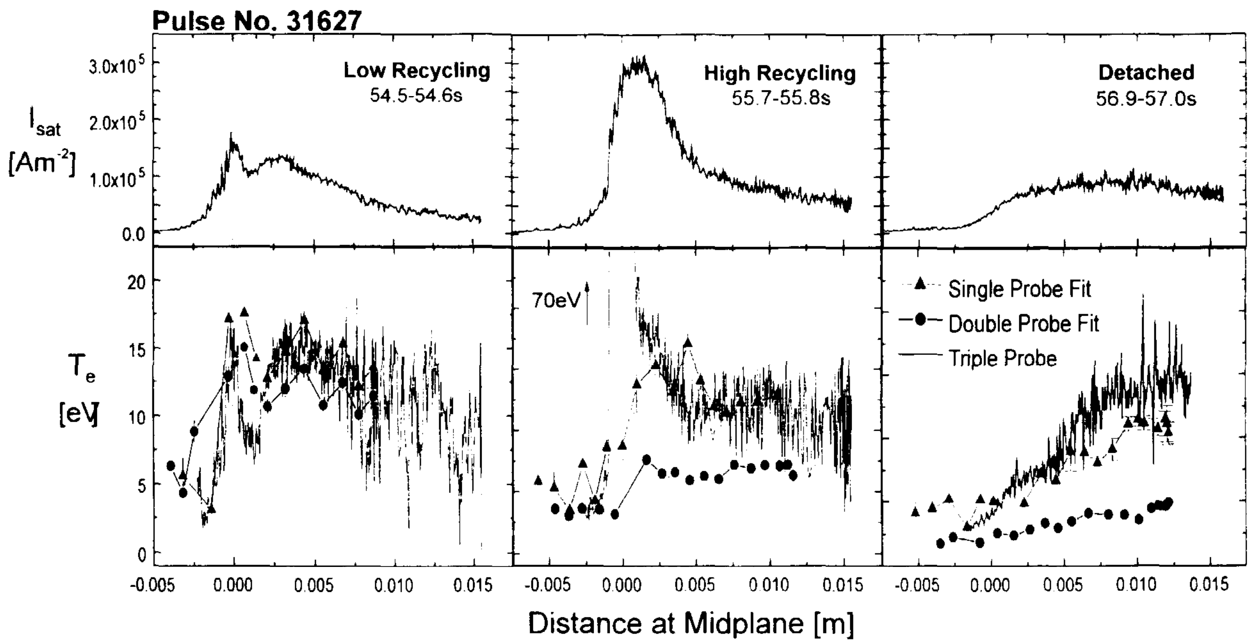
Pulse No. 31627
Low Recycling
54.5-54.6s
High Recycling
55.7-55.8s
Detached
56.9-57.0s
I_{sat}
[Am^{-2}]
3.0x10^5
2.0x10^5
1.0x10^5
0.0
T_e
[eV]
70eV
Single Probe Fit
Double Probe Fit
Triple Probe
Distance at Midplane [m]
-0.005
0.000
0.005
0.010
0.015

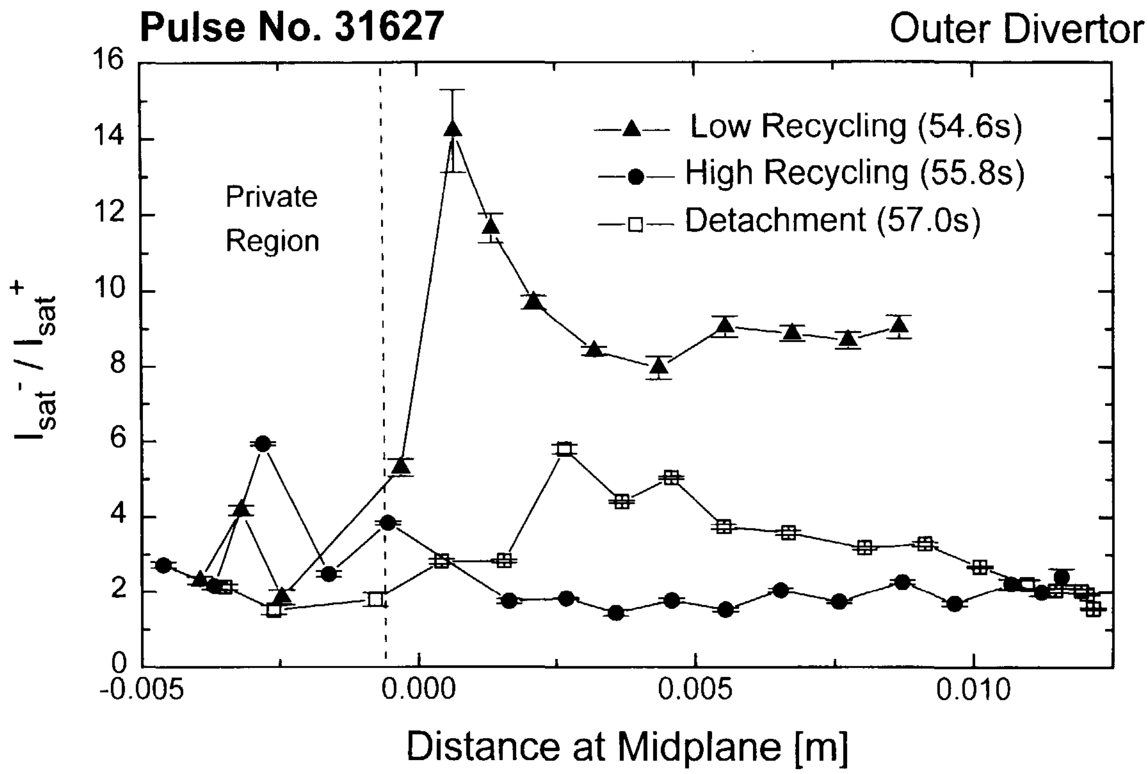
Pulse No. 31627
Outer Divertor
Private Region
Low Recycling (54.6s)
High Recycling (55.8s)
Detachment (57.0s)
I_{sat}^- / I_{sat}^+
Distance at Midplane [m]

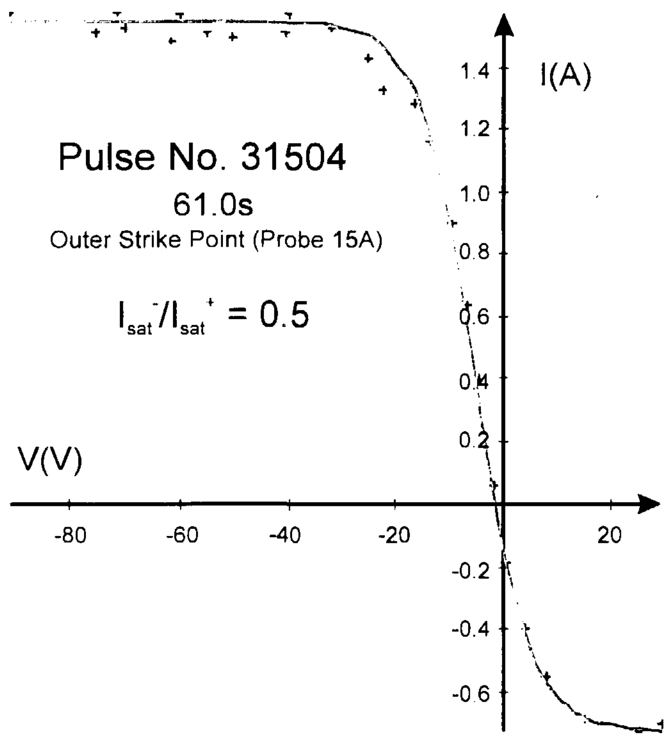
Pulse No. 31504
61.0s
Outer Strike Point (Probe 15A)
$I_{sat}^-/I_{sat}^+ = 0.5$
I(A)
V(V)

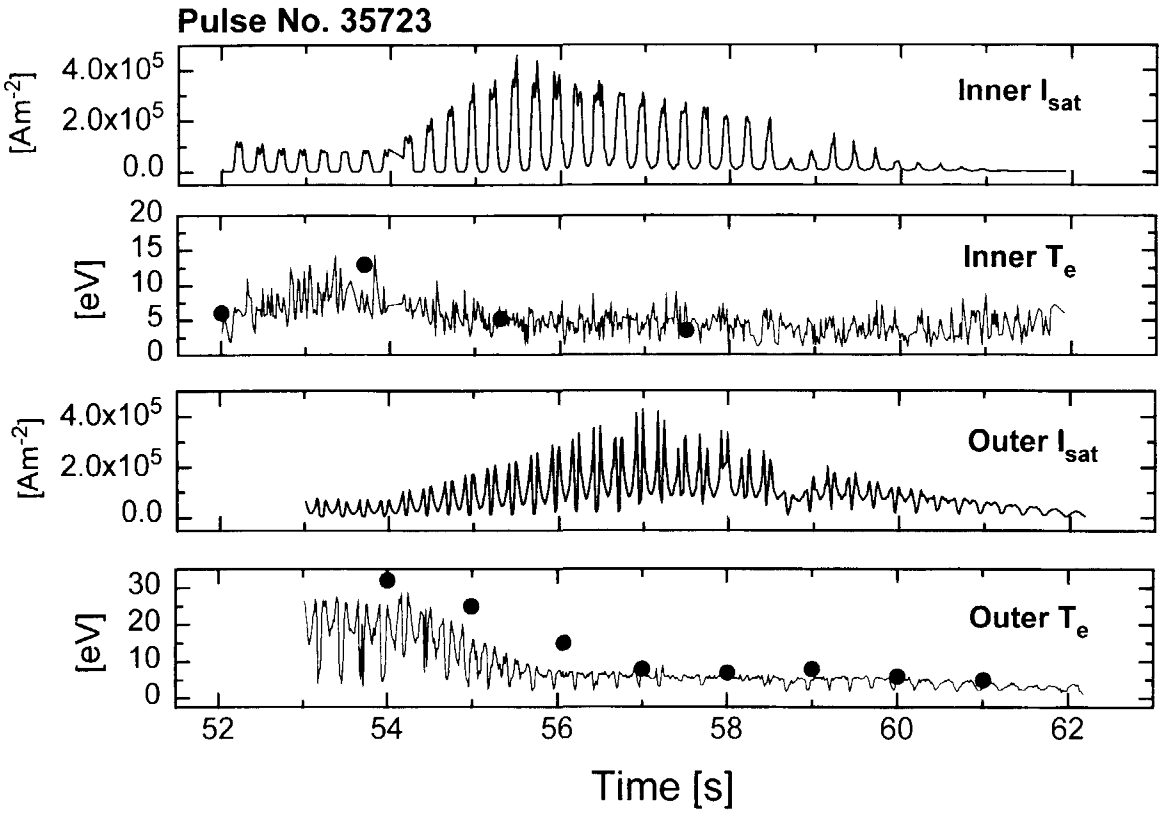

Pulse No. 35723
[Am^{-2}]
4.0x10^5
2.0x10^5
0.0
Inner I_{sat}
20
15
10
5
0
[eV]
Inner T_e
[Am^{-2}]
4.0x10^5
2.0x10^5
0.0
Outer I_{sat}
30
20
10
0
[eV]
Outer T_e
52
54
56
58
60
62
Time [s]